International Journal of Technology 15(4) 834-846 (2024)
Received October 2022 / Revised August 2023 / Accepted February 2024

International Journal of Technology

http://ijtech.eng.ui.ac.id

Optimal Design and Performance Analysis of Multiple Photovoltaic with Grid-Connected Commercial Load

Hanis Farhah Jamahori[1,2], Md Pauzi Abdullah[2*], Abid Ali[3], Abdulrahman AlKassem[4]

[1]*Faculty of Engineering, Built Environment and IT, Mahsa University, 42610 Selangor, Malaysia*
[2]*Institute of Future Energy, Faculty of Electrical Engineering, Universiti Teknologi Malaysia, 81310 Johor Bahru, Malaysia*
[3]*Interdisciplinary Institute of Technological Innovation (3IT), Université de Sherbrooke, 3000 Boulevard Université, Sherbrooke, J1K OA5 Québec, Canada*
[4]*Department of Electrical Engineering, Faculty of Engineering, Islamic University of Madinah, Madinah 42351, Saudi Arabia*

Abstract. This study aimed to evaluate the potential of integrating Photovoltaic (PV) with commercial load and examine the impact on distribution networks. To estimate the hourly PV output power, 13 years of historical weather data were used. Furthermore, a beta probability density function was modeled to handle large amounts of data and generate a 24-hour predicted PV curve. Particle Swarm Optimization (PSO) was used to determine the location and size of multiple PV units, ranging from 1 to 3. PV performance was tested on IEEE 33-bus and 69-bus test systems using time-varying commercial load, with power loss index (PLI) set as the objective function. PV penetration level was also calculated. The results showed a significant power loss reduction and PV penetration levels when 3 PV units were integrated into the system compared to a single PV unit. Specifically, the power loss reduction improved from 32.71% to 45.37% and 43.80% to 48.08%, producing PV penetration levels of 43.08% and 40.15% in 33-bus and 69-bus systems, respectively. The results indicated that the integration of multiple PV units was better than the single PV integration. The proposed model using PSO determined the impact of considering weather-dependent PV generation simultaneously with time-varying loads. It also provided knowledge to model the optimal location and sizing of multiple PV units in the distribution networks based on the generated solar irradiance patterns.

Keywords: Commercial load; Historical weather data; Power loss; PV penetration; Particle swarm optimization

1. Introduction

Distributed generation (DG) integration has significantly increased in recent years and is expected to continue expanding, playing a more prominent role in the future energy market. DG offers several advantages when integrated into a distribution system, significantly altering the parameters (Hassan *et al.*, 2020; Lee *et al.*, 2020; Kola, 2018). Moreover, some of the technical benefits include reducing transmission losses when connected near the consumer load, improving bus voltage profile and power quality, increasing system security and reliability, reducing dependency on the grid operator,

*Corresponding author's email: mpauzi@utm.my, Tel.: +607-5535896; Fax: +607-5566272
doi: 10.14716/ijtech.v15i4.6019

serving as a backup source of electricity in emergencies and meeting the demand for electricity in rural or remote areas (Zagloel *et al.,* 2023; Biswas *et al.,* 2017). Conventional diesel generators have traditionally been considered the most reliable and affordable DG source. However, environmental concerns and high fuel prices have imposed limitations on the usage. This concern has facilitated the adoption of renewable energy (RE) as an alternative DG source for power generation (Saroji *et al.,* 2022). RE-based DG technologies, known as distributed renewable energy generation, (DREG), include solar Photovoltaic (PV), wind turbines, biomass, tidal, and hydropower (Zheng *et al.,* 2021). The availability of RE in various countries worldwide and adequate energy resources have led to the growing interest due to the abundance and self-sustaining nature of these energy sources. Recently, there has been a tremendous increase in DREG installations in distribution networks. The main factors contributing to this trend are reductions in capital expenditure and operational costs, particularly for PV and wind, as well as the introduction of smart grid technologies fostering more flexible distribution of intermittent power in the grid (Zheng *et al.,* 2021; Kåberger, 2018). Among all available RE-based DG sources, PV has gained more popularity (Jung, Pagidipala, and Salkuti, 2024; Bhambri *et al.,* 2023; Diwania *et al.,* 2020). Furthermore, it is rapidly growing and being utilized as an alternative to conventional power generation using fossil fuels (Kumar *et al.,* 2023; Onibonoje, 2023; Sánchez *et al.,* 2023). Despite the unprecedented pandemic in 2019, global solar capacity remains dominant for newly installed power generation, reaching a 39% global market share. This has increased global cumulative solar capacity from 104 GW in 2012 to 1 TW in 2022 (IRENA, 2022; Solar Power Europe, 2022). Under optimal conditions, the projected global solar capacity is expected to reach 2 TW by 2025 (Board, 2022). Moreover, the advantage of utilizing PV system as a RE source is the derivation from nature and abundant availability of resources. PV has low maintenance and operational costs since power generation does not comprise mechanical moving parts (Zhao *et al.,* 2021; Lupangu and Bansal, 2017).

1.1. Literature Review

Several studies have focused on planning DREG technologies in distribution networks, with the aim of minimizing power losses and improving PV penetration through optimization. Various optimization methods have been used to determine the optimal size and location of DREG units in power systems, focusing on reducing transmission power losses and improving voltage profiles. (Khenissi *et al.,* 2021) proposed using PSO and GA methods to determine the optimal location and size of PV units. The study found that PSO outperformed GA in terms of convergence, reduced power loss, and better voltage profile. Similarly, the proposed Adaptive Particle Swarm Optimization (APSO) showed that APSO produced better accuracy, optimal solutions, and faster convergence than Bee Colony Optimization (BCO) and Lightening Search Algorithm (LSA). (Kumar, Nallagownden and Elamvazuthi, 2017) adopted a PSO algorithm for the optimal placement and sizing of DG units in a distribution system, with the aim of reducing power loss and improving voltage stability. The results confirmed the efficacy and robustness of PSO for PV integration in the distribution system. Furthermore, (Hassanzadeh and Jalilian, 2018) used PSO as a multi-objective optimization method for power loss reduction and voltage improvement in multi-DG placements in radial distribution systems. The results showed that PSO significantly reduced total losses of the distribution system and improved the voltage profile, producing optimal solutions with fast convergence. These studies generally showed that PSO not only saved costs but also produced lower power losses and better voltage profiles than Tabu Search, Hybrid, and GA.

Studies have examined DREG planning, focusing on time-varying DG generation and loads. For instance, (Khan, Malik, and Sajjad, 2018) conducted a comparative analysis of the

impact of time-varying PV generation on load models. Three years of solar irradiance data were used to predict hourly PV output through a novel probabilistic generation modelling approach. In addition, the optimal size and location of PV units were determined based on (Khan and Malik, 2017), which applied PSO for similar purpose. (Ahmed *et al.,* 2020) proposed using Salp Swarm Algorithm (SSA) in a 19-bus system to optimize the location and size of wind-based DG for different time-varying loads based on multi-objective functions. However, this study was limited due to the use of pre-defined load models and inability to report the use of historical weather data. (Hossain *et al.,* 2023) showed the importance of determining the optimal size for PV combined with energy storage to accommodate varying commercial loads. However, the analysis focused on the economic aspects and did not consider the maximum PV power contribution to the grid for various load users. This oversight raised concerns about potential stress on the grid, necessitating a more comprehensive approach to balance economic considerations with grid infrastructure impacts. (Jamahori, Abdullah, and Ali, 2023) found that optimizing PV generation by considering historical weather-dependent data and time-varying loads could effectively meet diverse load demands. However, the study was limited to the installation of a single PV unit, potentially compromising the attainment of optimal results and the determination of the most efficient PV unit required in the distribution network.

Based on existing literature, most studies used various optimization methods to determine the optimal size and location of DREG units in power systems, addressing different objective functions. However, there are still gaps in studies concerning variations in load demands and peak generation aspects. Addressing these gaps is crucial to approximate PV size accurately, prevent overgeneration during periods of low demand, and ensure sufficient electricity generation during peak hours. Therefore, the current study aimed to provide insights into how an optimized PV generation system performed effectively under changing load conditions and assessed the impact on the general distribution system. Evaluating varying load demands with PV integration is important, as it offers more accurate results for managing real-time daily load consumers in the future.

2. Problem Formulation

2.1. Solar PV Modelling

Thirteen years of hourly weather satellite data (Solcast, 2018) were used to forecast the average hourly irradiance and PV output power as well as evaluate the potential of PV integration with commercial loads in Malaysia (30821N, 1014113E). The location of Malaysia near the equatorial makes it a perfect opportunity to utilize abundant solar energy resources, with an average annual irradiance of 4-5 kWh/m^2/day (Mohammad, Al-Kayiem, and Aurybi, 2020). The historical data collected were divided into 24-hour segments, each with solar irradiance measured at specific hours. The mean (μ) and standard deviation (σ) for each hour were calculated based on the irradiance data collected hourly over the 13 years. This facilitated the determination of the probability of solar irradiance for each hour and the estimation of PV output. The Beta-PDF f(s) is expressed using equation (1) as follows (Atwa *et al.,* 2010):

$$f(s) = \begin{cases} \dfrac{\Gamma(\alpha+\beta)}{\Gamma(\alpha)\ x\ \Gamma(\beta)},\ s^{(\alpha-1)}\,(1-s)^{(\beta-1)}, & 0 \le s \le 1, \alpha, \beta \ge 0 \\ 0 & \text{otherwise} \end{cases} \quad (1)$$

where s is a random variable for solar irradiance measured in (kW/m^2), Γ is a gamma function, α and β both parameters of equation (6) are derived using mean, μ and standard deviation, σ respectively using equation (2) (Atwa *et al.,* 2010):

$$\alpha = \frac{\mu \times \beta}{(1+\mu)}; \qquad \beta = (1-\mu)\left(\frac{\mu\,(1+\mu)}{\sigma^2} - 1\right) \tag{2}$$

The probability of solar irradiance, s in the limits of s1 and s2 during a specific hour (t=1) can be obtained using equation (3) (Atwa *et al.,* 2010):

$$p(s) = \int_{s2}^{s1} f(s)\, ds \tag{3}$$

2.2. PV Module Output

PV power is significantly influenced by temperature, climate and geographical factors, and solar irradiance. The output of PV module, PV_{NET} is expressed as a function of solar irradiance as follows (Atwa *et al.,* 2010):

$$PV_{NETt}(s) = N \times FF \times V_{NET} \times I_{NET} \tag{4}$$

$$FF = \frac{V_{MPPT} \times I_{MPPT}}{V_{OC} \times I_{SC}} \tag{5}$$

$$V_{NET} = V_{OC} - K_V \times T_C \tag{6}$$

$$I_{NET} = s \times [I_{SC} + K_i\, x\, (T_C - 25)] \tag{7}$$

$$T_C = T_A + s\left(\frac{N_{OT} - 20}{0.8}\right) \tag{8}$$

where N is the number of PV modules, and FF is the fill factor that depends on solar irradiance. The total expected PV output power at a given hour, $PV_{out}(t)$ at (t = 1 hour), is derived using (3) and (4), which relies on the irradiance s, and the characteristic of the modules given by equation (5)-(8) is expressed by the following expression equation (9) (Ali *et al.,* 2018):

$$PV_{out}(t) = \int_0^1 PV_{NET}\,(s)\, p(s)\, ds \tag{9}$$

2.3. Load Modelling

The following equations (10)-(11) express the new active and reactive distribution load demand $P_{Dnew,i}$ and $Q_{Dnew,i}$ at a respective bus integrated with time-varying commercial loads in a given period (t) equation (Atwa *et al.,* 2010):

$$P_{Dnew,i}\,(t) = P_{Di}\,(t) \times V_i^{vp}(t) \tag{10}$$

$$Q_{Dnew,i}(t) = Q_{Di}\,(t) \times V_i^{vq}(t) \tag{11}$$

where, P_{Di}, and Q_{Di} are the actual active and reactive load power and V_i is voltage magnitude at i bus calculated under base caseload conditions. The active and reactive voltage exponential, vp and vq are 1.51 and 3.40, respectively, for time-varying voltage-dependent commercial loads (Nor *et al.,* 2018). Figure 1 shows the normalized load curve for the commercial model, with a peak magnitude of 1.00 (p.u).

2.4. Distribution Bus System

This study used a standard IEEE 33-bus and 69-bus test system, with each distribution bus having different load power and system losses. The rated voltage for both systems was 100 MVA and 12.66 kV. The total load demand and base power losses for 33-bus were 3.715 MW, 2.300 MVAr, and 211.20 kW, 143.03 kVAr, respectively. The total load demand and base power losses for 69-bus were 3.800 MW, 2.690 MVAr, and 224.95 kW, 102.14 kVAr, respectively (Kakueinejad *et al.,* 2020; Nawaz and Tandon, 2018). Furthermore, both bus

systems were assumed to serve as distribution power stations for commercial load areas, meaning that all connection points were considered commercial consumers. This study was limited to using historical weather data based on collected solar irradiation, acknowledging that the power output might vary depending on solar irradiation at a specific location. It was assumed that the distribution grid was connected to the commercial load areas.

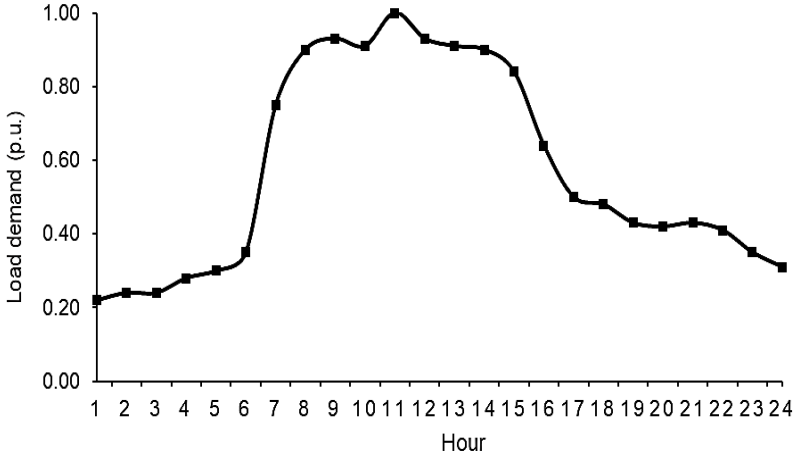

Figure 1 The normalized commercial load curve (Jamahori, Abdullah and Ali, 2023)

2.5. Load Flow Analysis

Assuming 2 buses, k and k + 1 connected through branch i, the following formula equation (12)-(13) was used to calculate the active, $P_{Loss(i)}$ and reactive, $Q_{Loss(i)}$ branch power loss between 2 buses (Ali *et al.,* 2018):

$$P_{Loss(i)} = R_i \left(\frac{{P_{k+1}}^2 + {Q_{k+1}}^2}{|V_{k+1}|^2} \right) \quad (12)$$

$$Q_{Loss(i)} = X_i \left(\frac{{P_{k+1}}^2 + {Q_{k+1}}^2}{|V_{k+1}|^2} \right) \quad (13)$$

where R_{ij} is the branch resistance and X_{ij} is the branch reactance between 2 buses. The base case (without PV) hourly active and reactive power injection across any branches at each period can be calculated as a summation of effective $k + 1^{th}$ bus power, load demand power, and power losses at k + 1 bus as follows equation (14)-(15) (Ali *et al.,* 2018):

$$P_{(i)}(t) = P_{(k+1)}(t) + P_{D(k+1)}(t) + P_{Loss(i)}(t) \quad (14)$$

$$Q_{(i)}(t) = Q_{(k+1)}(t) + Q_{D(k+1)}(t) + Q_{Loss(i)}(t) \quad (15)$$

where P_i, and $Q_{(i)}$ are the active and reactive power injections between 2 buses, with $P_{D(ij)}$ and $Q_{D(ij)}$ as the actual load power between both buses. The total power losses, $TP_{Loss(i)}$ before PV integration are a summation of both losses given by equation (16) derived from equation (12) and equation (13):

$$TP_{Loss(i)} = \sum_{i=1}^{N_{branches}} (P_{Loss(i)} + jQ_{Loss(i)}) \quad (16)$$

2.6. PV Integrated System

The addition of a new power source affected the load flow in the distribution system. Therefore, the new active, $P_{Dnew(k+1)}$ and reactive, $Q_{Dnew(k+1)}$ power injections at k + 1 bus, where PV is installed, are as follows equation (17)-(18) (Ali *et al.,* 2018):

$$P_{Dnew(k+1)} = P_{PV} - P_{D(k+1)} \quad (17)$$

$$Q_{Dnew(k+1)} = Q_{PV} - Q_{D(k+1)} \quad (18)$$

where $P_{D(k+1)}$ and $Q_{D(k+1)}$ are the actual active and reactive load power at the effective bus, while P_{PV} and Q_{PV} are the active and reactive power generation from PV. Q_{PV} is a function of P_{PV} with a fixed power factor, therefore, $Q_{PV} = a\,P_{PV}$, where $a = \pm\tan\{\cos^{-1}(pf(P_{PVi}))\}$, a is positive (+) when PV injects reactive power and negative (-) when it consumes reactive power, and pf is an operating power factor of PV unit at bus $k + 1$.

Assuming the solar PV unit is installed at $k + 1$ bus, the hourly active, $P_{(i)}(t)$ and reactive, $Q_{(i)}(t)$ power injection across branch i at each period can be calculated as follows equation (19)-(20) (Jamahori, Abdullah and Ali, 2023):

$$P_{(i)}(t) = P_{(k+1)}(t) + P_{D(k+1)}(t) + P_{Loss(i)}(t) - P_{PV}(t) \quad (19)$$

$$Q_{(i)}(t) = Q_{(k+1)}(t) + Q_{D(k+1)}(t) + Q_{Loss(i)}(t) - Q_{PV}(t) \quad (20)$$

The new power loss, $P_{Loss,PV(i)}$ and $Q_{Loss,PV(i)}$ in any branches after PV is connected at $k + 1$ bus can be calculated using equation (21)-(22) (Jamahori, Abdullah and Ali, 2021):

$$P_{Loss,PV(i)} = R_i\left(\frac{(P_{(k+1)} - P_{PV})^2 + (Q_{(k+1)} - Q_{PV})^2}{|V_{k+1}|^2}\right) \quad (21)$$

$$Q_{Loss,PV(i)} = X_i\left(\frac{(P_{(k+1)} - P_{PV})^2 + (Q_{(k+1)} - Q_{PV})^2}{|V_{k+1}|^2}\right) \quad (22)$$

Similarly, the new total losses, $TP_{Loss,PV(i)}(t)$ in all branches after the installation of PV at $k + 1$ bus at each period are calculated using equation (23) (Jamahori, Abdullah and Ali, 2021):

$$TP_{Loss,PV(i)}(t) = \sum_{i=1,\ t=1}^{N_{branches},\,t=24} (P_{Loss,PV(i)}(t) + jQ_{Loss,PV(i)}(t) \quad (23)$$

This study aimed to minimize the overall power loss. Therefore, power loss index (PLI) was set as the objective function f. PLI can be defined as the ratio of losses with PV to the base case power losses without PV (24), which is the ratio between equation (23) and (16) with the time-varying commercial load as follows (Jamahori, Abdullah and Ali, 2021):

$$f, PLI = \min \sum_{t=1}^{t=24} \frac{TP_{Loss,PV(i)}}{TP_{Loss(i)}} \quad (24)$$

2.7. Particle Swarm Optimization (PSO)

PSO algorithm-based random particle generation aimed to achieve the best value of the fitness function by updating the position and velocity. The basic principle of PSO works by using the swarm's knowledge and experience to randomly direct particles across the search space to find the best local and global solution, g_best based on their personal best solution, p_best. The particles change by updating position and velocity using a weighted acceleration, ω, at each iteration to accelerate toward the fitness function. PSO updates each particle by comparing the best fitness to the current p_{best}. Assuming the new generation of fitness is superior to the current p_{best}, newly generated fitness replaces p_{best} solution. Finally, the best global solution for any particle, g_{best} is selected by comparing all particles' fitness. The flowchart of the optimization framework using PSO is shown in Figure 2.

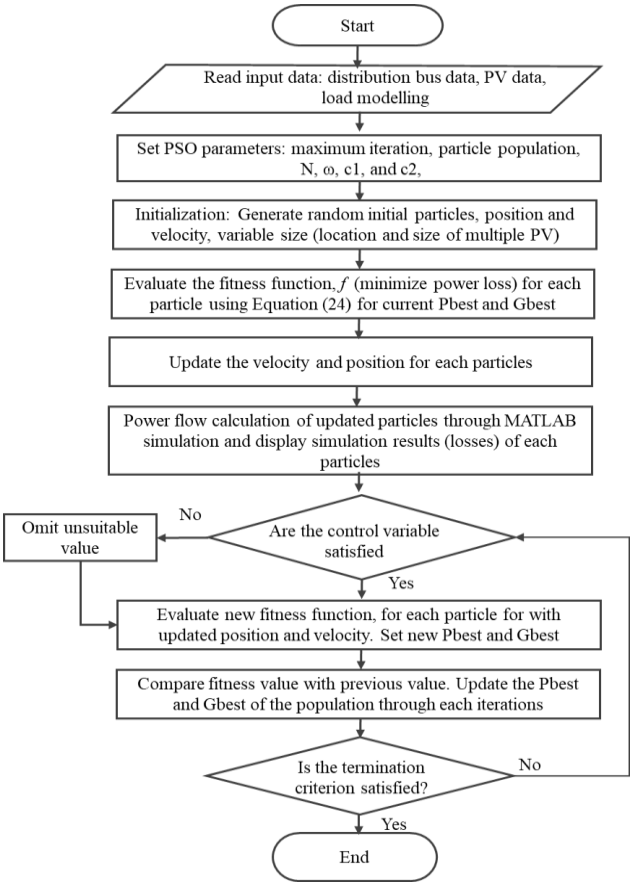

Figure 2 The flowchart of the optimization framework using PSO

PSO parameters were selected based on initial suggestions from the year of development (1995), which proposed limiting the population size to 20-50 particles. Larger swarms typically improved the efficiency of the method for more complicated problems and practical applications. While significantly smaller swarm sizes were suggested for the majority of PSO variants regarding unimodal problems, hundreds of particles/swarms would still perform optimally. PSO parameters for the integration of multiple PV are shown in Table 1.

Table 1 PSO Parameters for integration of multiple PV

Parameters	Value/Type
Fitness function	*f*, Power loss index (PLI)
Variable size	Location and size
Population size	50-100
No. of iteration	100
c_1, c_2	1.05, 1.05
ω_{min}, ω_{max}	1.0, 0.3

3. Results and Discussion

3.1. Optimal Location and Size of Multiple PV units

The simulation result for multiple PV integrations with commercial load users in IEEE 33-bus and IEEE 69-bus are summarized in Tables 2 and 3, respectively. Based on the optimization, the results showed that the optimal PV sizing for the commercial load users differed significantly in both distribution networks. This was mainly due to the optimal location and power demand in each bus system.

Tabel 2 Summary of multiple PV optimization results in IEEE 33-Bus

Parameters	Without PV	1PV	2PV	3PV
PV Location @		6 @ 4.57	12 @ 1.71	14 @ 1.41
PV Size (MW)			30 @ 2.08	24 @ 1.75,
				30 @ 1.75
Total PV Size (MW)		4.57	3.79	4.91
PLoss (kW)	1952.14	1313.54	1158.36	1066.38
PLoss Reduction, %		32.71	40.66	45.37
QLoss (kVAr)	1322.56	931.81	789.84	729.95
QLoss Reduction, %		29.54	40.28	44.81
PV Penetration, %		40.15	33.29	43.08

Tabel 3 Summary of multiple PV optimization results in IEEE 69-Bus

Parameters	Without PV	1PV	2PV	3PV
PV Location @		61 @ 3.35	18 @ 0.99	11 @ 0.91
PV Size (MW)			61 @ 3.19	17 @ 0.72
				61 @ 3.04
Total PV Size (MW)		3.35	4.18	4.67
PLoss (kW)	2074.32	1165.83	1091.18	1076.94
PLoss Reduction, %		43.80	47.40	48.08
QLoss (kVAr)	943.79	548.60	518.76	512.78
QLoss Reduction, %		41.87	45.03	45.67
PV Penetration, %		28.72	35.90	40.15

For IEEE 33-bus, the optimal PV integration for a single PV was at bus 6 with a size of 4.57 MW, while 2 PV units were at bus 12 and 30, respectively, with a size of 1.71 MW and 2.08 MW. The optimal location and sizing of 3 PV units were at bus 14, 24, and 30, with PV sizes of 1.41 MW, 1.75 MW, and 1.75 MW, respectively. In IEEE 69-bus, the optimal PV integration for a single PV was at bus 61 with the size of 3.35 MW, while 2 PV units were at buses 18 and 61, respectively, with the size of 0.99 MW and 3.19 MW. The optimal location and sizing of 3 PV units were at buses 11, 17, and 61, with PV sizes of 0.91 MW, 0.72 MW, and 3.04 MW, respectively. The cumulative PV sizes for 1, 2, and 3 PV units were 4.57 MW, 3.79 MW, and 4.91 MW, respectively, for IEEE 33-bus and 3.35 MW, 4.18 MW, and 4.67 MW, respectively, for IEEE 69-bus. The results showed that the average total PV size was larger when integrated with commercial load users in 33-bus compared to 69-bus system.

Figure 3 presents the expected PV output from Equation (9) and commercial demand consumption for both systems using Equations (10) and (11). Furthermore, maximum PV production and load consumption occurred concurrently during the day, following the solar PV production, which peaked at noon and was low in the morning and evening.

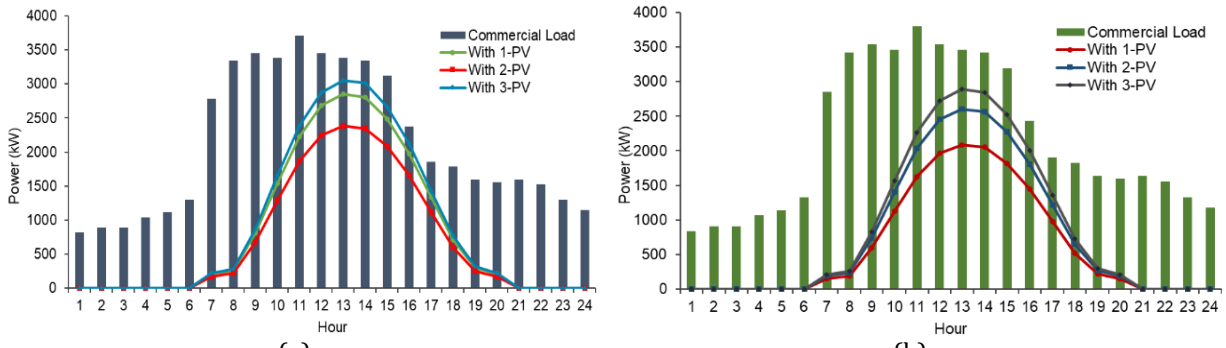

Figure 3 Expected PV output with commercial demand (a) IEEE 33-Bus; and (b) IEEE 69-Bus

Since the system operated as an integrated grid system, the grid served the remaining load consumption when PV power was unavailable or insufficient to supply the load. On the other hand, the highest PV output was observed when 3 PV units were integrated into both bus systems. The expected PV output was lowest with 2 PV in 33-bus and 1 PV unit in 69-bus system. While the varying lowest PV size between both buses did not affect the overall power losses, it affected the overall PV penetration. Further discussion on PV penetration level and power loss reduction was provided in the next sub-section.

3.2. Impact on PV Penetration

PV penetration level is the total expected PV output (MW) ratio to the total load demand consumed during the day (MW). A high penetration level shows that PV production is sufficient to provide power to meet the load demand. PV penetration results are presented in Figure 4. Based on the results, PV penetration levels for 1, 2, and 3 PV units in 33-bus and 69-bus were 40.15%, 33.29%, 43.08%, and 28.72%, 35.90%, 40.15%, respectively.

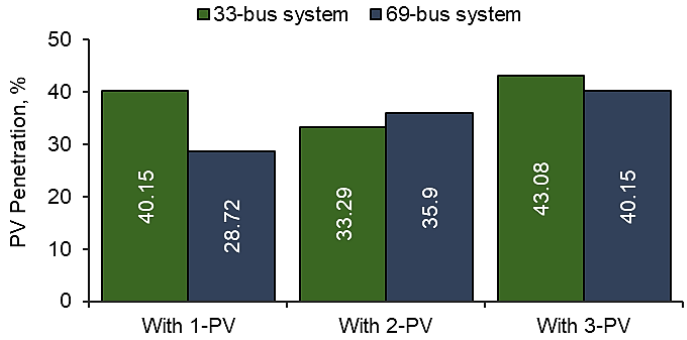

Figure 4 Penetration level for multiple PV integration

The penetration level increased significantly with load demand in 69-bus as the number of installed PV increased, while the difference in penetration level between 1 PV and 3 PV in 33-bus was insignificant. The maximum PV penetration was recorded when 3 PV units were integrated with commercial load in 33-bus, and the least being 1 unit integrated into 69-bus system. As mentioned, the optimum size of PV was subjected to power loss minimization. Since power loss in the distribution system depended on the load of each model, the size of PV units in each case varied accordingly. The cumulative sizes of PV in MW for each load model considering single and multiple PV units for the two distribution systems are presented in Tables 2 and 3. For 33-bus system, the impact of 2 PV units on the total size of PV in MW was the most optimal compared to the installation of 1 and 3 PV units. On the other hand, for 69-bus distribution system, the impact of 1 PV unit on the total size of PV in MW was more optimal than the installation of 2 and 3 PV units. Therefore, the penetration of PV units in the distribution networks varied and depended on the size of PV in distribution networks.

3.3. Impact on Power Losses

The power loss for multiple PV integration in both buses is presented in Figure 5. The power loss reduction showed promising results after multiple PV units were integrated into both bus systems. Specifically, the power loss for 1, 2, and 3 PV units in 33-bus and 69-bus were 32.71%, 40.66%, 45.37%, and 43.80%, 47.40%, 48.08%, respectively. These power losses were influenced by the total PV generated during the day, the total load served at a specific hour, and the location and sizing of PV units. In addition, the load demand variations in each bus directly affected the location for PV installation. This could be attributed to the typical installation of PV near areas with the highest load demand and farther from the grid supply to ensure continuous power supply while minimizing voltage

deviation and power loss. The reduction in power losses was more significant with multiple PV in 33-bus compared to 69-bus system. The installation of a third PV in 69-bus did not significantly reduce the total power losses. Therefore, 3 PV units were more optimal to be installed for 33-bus, and only 2 PV units were recommended for time-varying commercial users in 69-bus system, as the effect of the third PV could be neglected. This was because the rate of improvement in distribution system performance was primarily determined by the total size of PV units.

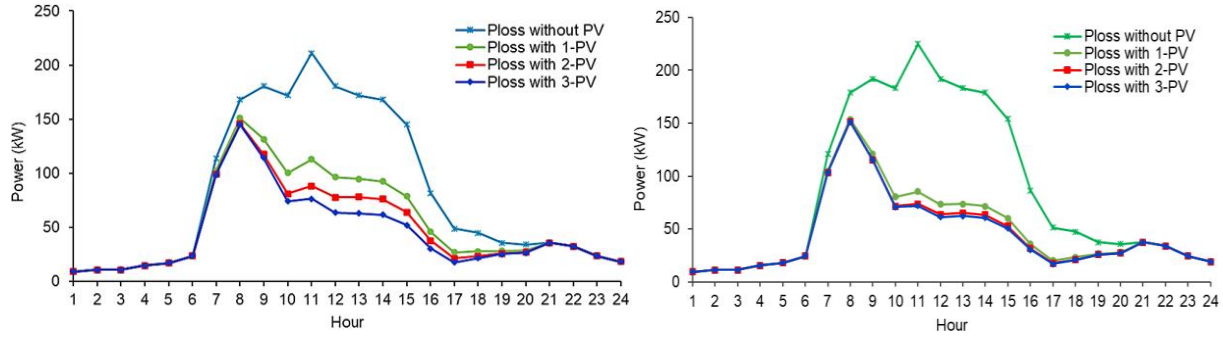

Figure 5 Power loss for multiple PV integration (a) IEEE 33-Bus; and (b) IEEE 69-Bus

The optimal location and size of 1 to 3 PV units were determined based on proximity to areas with the highest load demand and distance from the grid supply. This ensured the additional sources from PV could continue to supply the load at a different location. The power losses with multiple PV were affected by the total PV generated during the day, the total load served at a specific hour, and the total PV sizing on the individual location. In addition, the load demand variations in different bus systems directly affected the location of installation. Integrating multiple PV units showed that beyond installing 2 PV units, there was no significant impact on 69-bus system. However, installing 3 PV was significant in addressing the load demand in 33-bus system. The reduction in power losses was more prominent within 33-bus compared to 69-bus system. The power loss was influenced by the supply of power to the distribution networks and depended on the size of PV units. Larger PV sizes corresponded with greater improvements in bus voltage magnitude. Nonetheless, inadequate PV sizing could lead to additional power losses and suboptimal improvement of bus voltage profiles.

4. Conclusions

In conclusion, this study showed that modeling multiple PV units with commercial load users at optimal size and location had varied impacts on the distribution system performance. Furthermore, the integration of multiple PV units outperformed single PV integration, resulting in improved power loss reduction from 32.71% to 45.37% and 43.80% to 48.08% in 33-bus and 69-bus systems, respectively. This integration produced PV penetration levels of 43.08% and 40.15% in the respective bus systems. The proposed model not only assessed the impact of considering weather-dependent PV generation alongside time-varying loads but also provided insights into modeling the optimal location and sizing of multiple PV units in distribution networks based on solar irradiance patterns. Moreover, this study showed the importance of considering load variations in designing a PV grid system to ensure optimal performance and efficiency. By accounting for variations in load demand, PV system could be appropriately sized to match varying load profiles, preventing overgeneration during low-demand periods and ensuring sufficient electricity

generation during peak hours. This method maximized the utilization of renewable energy and helped to maintain grid stability and reliability, ensuring consistent voltage levels, balanced power flow, and the ability to respond swiftly to changes in demand or supply to minimize power losses. Therefore, considering load variations was essential for the successful and resilient operation of PV grid system.

References

Ahmed, A., Nadeem, M.F., Sajjad, I.A., Bo, R., Khan, I.A., 2020. Optimal Allocation of Wind DG with Time Varying Voltage Dependent Loads Using Bio-Inspired: Salp Swarm Algorithm. *In:* 3rd International Conference on Computing, Mathematics and Engineering Technologies (iCoMET)

Ali, A., Nor, N. M., Ibrahim, T., Romlie, M.F., 2018. Sizing and Placement of Solar Photovoltaic Plants by Using Time-Series Historical Weather Data. *Journal of Renewable and Sustainable Energy,* Volume 10(2), p. 023702

Atwa, Y.M., El-Saadany, E.F., Salama, M.M.A., Seethapathy, R., 2010. Optimal Renewable Resources Mix for Distribution System Energy Loss Minimization. *IEEE Transactions on Power Systems,* Volume 25(1), pp. 360–370

Bhambri, S., Kumawat, M., Shrivastava, V., Agarwal, U., Jain, N.K., 2023. The Energy Mix: An Emerging Trend in Distribution System. *Optimal Planning and Operation of Distributed Energy Resources*. Spinger

Biswas, P.P., Mallipeddi, R., Suganthan, P.N., Amaratunga, G.A.J., 2017. A Multiobjective Approach for Optimal Placement and Sizing of Distributed Generators and Capacitors in Distribution Network. *Applied Soft Computing,* Volume 60, pp. 268–280

Board, T.C., 2022. Global Economic Outlook. Available onlie at: https://www.conference-board.org/topics/global-economic-outlook, Accessed on Agustus 31, 2022

Diwania, S., Agrawal, S., Siddiqui, A.S., Singh, S., 2020. Photovoltaic–thermal (PV/T) Technology: A Comprehensive Review on Applications and Its Advancement. *International Journal of Energy and Environmental Engineering,* Volume 11(1), pp. 33–54

Hassan, A.S., Othman, E.A., Bendary, F.M., Ebrahim, M.A., 2020. Optimal Integration of Distributed Generation Resources in Active Distribution Networks for Techno-Economic Benefits. *Energy Reports,* Volume 6, pp. 3462–3471

HassanzadehFard, H., Jalilian, A., 2018. Optimal Sizing and Siting of Renewable Energy Resources in Distribution Systems Considering Time Varying Electrical/Heating/Cooling Loads Using PSO Algorithm. *International Journal of Green Energy,* Volume 15(2), pp. 113–128

Hossain, J., Kadir, A.F.A., Shareef, H., Manojkumar, R., Saeed, N., Hanafi, A.N., 2023. A Grid-Connected Optimal Hybrid PV-BES System Sizing for Malaysian Commercial Buildings. *Sustainability,* Volume 15(13), p. 10564

IRENA, 2022. Latest Trend in Renewable Energy. Available online at https://www.irena.org/Statistics/View-Data-by-Topic/Capacity-and-Generation/Statistics-Time-Series, Accessed on August 31, 2022

Jamahori, H.F., Abdullah, M.P., Ali, A., 2021. Integration of PV Distributed Renewable Energy Generation into Distribution System using Time-Varying Weather and Load Data. *In:* IEEE 19th Student Conference on Research and Development (SCOReD)

Jamahori, H.F., Abdullah, M.P., Ali, A., 2023. Impact and Evaluation of Optimized PV Generation in the Distribution System with Varying Load Demands. *Jurnal Teknologi,* Volume *85*(3), pp. 61–73

Jung, C.-M., Pagidipala, S., Salkuti, S.R., 2024. Emerging Technologies for the Integration of Renewable Energy, Energy Storage and Electric Vehicles. *Energy and Environmental Aspects of Emerging Technologies for Smart Grid*. Springer

Kåberger, T., 2018. Progress of Renewable Electricity Replacing Fossil Fuels. *Global Energy Interconnection,* Volume 1(1), pp. 48–52

Kakueinejad, M., Heydari, A., Askari, M., Keynia, F., 2020. Optimal Planning for the Development of Power System in Respect to Distributed Generations Based on the Binary Dragonfly Algorithm. *Applied Sciences,* Volume 10(14), p. 4795

Khan, M.F.N., Malik, T.N., 2017. Probablistic Generation Model For Optimal Allocation of PV DG In Distribution System with Time-Varying Load Models. *Journal of Renewable and Sustainable Energy,* Volume 9(6), p. 065503

Khan, M.F.N., Malik, T.N., Sajjad, I.A., 2018. Impact of Time Varying Load Models on PV DG Planning. *Journal of Renewable and Sustainable Energy,* Volume 10(3), p. 035501

Khenissi, I., Sellami, R., Fakhfakh, M.A., Neji, R., 2021. Power Loss Minimization Using Optimal Placement and Sizing of Photovoltaic Distributed Generation Under Daily Load Consumption Profile with PSO and GA Algorithms. *Journal of Control, Automation and Electrical Systems,* Volume 32, pp. 1317–1331

Kola, S.S., 2018. A Review on Optimal Allocation and Sizing Techniques for DG in Distribution Systems. *International Journal of Renewable Energy Research,* Volume 8, pp. 1236–1256

Kumar, C.M.S., Singh, S., Gupta, M.K., Nimdeo, Y.M., Raushan, R., Deorankar, A.V., Kumar, T.M.A., Rout, P.K., Chanotiya, C.S., Pakhale, V.D., Nannaware, A.S., 2023. Solar Energy: A Promising Renewable Source for Meeting Energy Demand in Indian Agriculture Applications. *Sustainable Energy Technologies and Assessments,* Volume 55, p. 102905

Kumar, M., Nallagownden, P., Elamvazuthi, I., 2017. Multi-Objective PSO Based Optimal Placement of Solar Power DG n Radial Distribution System. *Journal of Electrical Systems,* Volume 13, pp. 322–331

Lee, J.Y., Verayiah, R., Ong, K.H., Ramasamy, A.K., Marsadek, M.B., 2020. Distributed Generation: A Review on Current Energy Status, Grid-Interconnected PQ Issues, and Implementation Constraints of DG in Malaysia. *Energies,* Volume 13(24), p. 6479

Lupangu, C., Bansal, R.C., 2017. A Review of Technical Issues on the Development of Solar Photovoltaic Systems. *Renewable and Sustainable Energy Reviews,* Volume 73, pp. 950–965

Mohammad, S.T., Al-Kayiem, H.H., Aurybi, M.A., Khlief, A.K., 2020. Measurement of Global and direct Normal Solar Energy Radiation in Seri Iskandar and Comparison with Other Cities of Malaysia. *Case Studies in Thermal Engineering,* Volume 18, p. 100591

Nawaz, S., Tandon, A., 2018. Power Loss Minimisation of Rural Feeder of Jaipur City by Renewable-based DG Technologies. *Australian Journal of Electrical and Electronics Engineering,* Volume 15, pp. 1–8

Nor, N.M., Ali, A., Ibrahim, T., Romlie, M.F., 2018. Planning of Distributed Renewable Energy Resources Using Genetic Algorithm. In: *Sustainable Electrical Power Resources through Energy Optimization and Future Engineering,* S.A. Sulaiman, R. Kannan, S.A.A. Karim, N. Mohd Nor (Eds.). Springer

Onibonoje, M.O., Alegbeleye, O.O., Ojo, A.O., 2023. Control Design and Management of a Distributed Energy Resources System. *International Journal of Technology,* Volume 14(2), pp. 291–319

Sánchez, A.S., Junior, E.P., Gontijo, B.M., de Jong, P., dos Reis Nogueira, I.B., 2023. Replacing fossil fuels with renewable energy in islands of high ecological value: The cases of

Galápagos, Fernando de Noronha, and Príncipe. *Renewable and Sustainable Energy Reviews,* Volume 183, p. 113527

Saroji, G., Berawi, M.A., Sari, M., Madyaningarum, N., Socaningrum, J.F., Susantono, B., Woodhead, R., 2022. Optimizing the Development of Power Generation to Increase the Utilization of Renewable Energy Sources. *International Journal of Technology,* Volume 13(7), pp. 1422–1431

Solar Power Europe, 2022. Global Market Outlook For Solar Power 2022-2026. Available online https://www.solarpowereurope.org/insights/market-outlooks/global-market-outlook-for-solar-power-2022, Accessed data on July 25, 2022

Solcast, 2018. Solar Irradiance Data. Available online https://solcast.com/solar-radiation-data/, Accessed on March 20, 2022

Zagloel, T.Y.M., Harwahyu, R., Maknun, I.J., Kusrini, E., Whulanza, Y., 2023. Developing Models and Tools for Exploring the Synergies between Energy Transition and the Digital Economy. *International Journal of Technology,* Volume 14(8), pp. 291–319

Zhao, L., Jerbi, H., Abbassi, R., Liu, B., Latifi, M., Nakamura, H., 2021. Sizing Renewable Energy Systems With Energy Storage Systems Based Microgrids For Cost Minimization Using Hybrid Shuffled Frog-Leaping and Pattern Search Algorithm. *Sustainable Cities and Society,* Volume 73, p. 103124

Zheng, D., Zhang, W., Alemu, S.N., S., Wang, P., Bitew, G.T., Wei, D., Yue, J., 2021. Chapter 1 - The concept of microgrid and related terminologies. *Microgrid Protection and Control*. Academic Press